Research Article

Ahmed Umar*, John T.S. Irvine

Gasification of Glycerol Over Ni/γ-Al_2O_3 For Hydrogen Production: Tailoring Catalytic Properties to Control Deactivation

https://doi.org/10.1515/cse-2020-0006
received June 29, 2020; accepted September 15, 2020.

Abstract: The effects of catalyst loading, calcination and reaction temperatures on the structural properties and catalytic behavior of Ni/γ-Al_2O_3 catalyst system in relation to steam reforming of glycerol and catalyst deactivation were investigated. The results showed that catalyst loading, reaction and calcination temperatures had a profound influence on the structure and catalytic activity in glycerol conversion. Use of high calcination temperature (900-1000 °C) led to phase transformation of the active Ni/Al_2O_3 to less active spinel specie $NiAl_2O_4$ that resulted in a successive change of texture and color. The particle size growth and phase change at this temperature were responsible for the catalyst deactivation and low performance especially among the catalyst calcined at high temperatures. Conversely, at low reaction temperatures, catalyst surfaces were marred by carbon deposition. Whilethe polymeric carbon deposited at metal-support interface was associated with low reaction temperatures, high reaction temperatures were characterized predominantly by both amorphous carbon deposited on the active metal surface and polymeric or graphitic carbon deposited at metal-support interface respectively. Calcination temperature showed no significant influence on the location and type of coke deposited on the catalyst surface. Hence, catalyst loading, calcination and reaction temperatures could be tailored to enhance structural and catalytic properties and guard against catalyst deactivation.

Keywords: Steam Reforming; Biomass Feedstock; Gaseous Biofuel; Supported Catalyst; Fuel Cell; Coking

***Corresponding author: Ahmed Umar,** Department of Chemistry, University of Abuja, Gwagwalada, FCT, Abuja, Nigeria, E-mail: u.ahmed2007@yahoo.com
John, T.S.I. Irvine, School of Chemistry, University of St Andrews, North Haugh, St Andrews, Fife KY16 9ST, UK

1 Introduction

The demand for energy will inevitably be on the rise considering the exponential growth in world population and rapid industrialization. Fossil fuels (largely petroleum) which are the most predominant and major energy resource in the world are depleting rapidly and are unevenly distributed around the globe; they are responsible for environmental issues affecting the world today. Such issues include atmospheric pollution, global warming, climate change, toxicity, non-biodegradability, and energy insecurity [1]. The Solid Oxide Fuel Cell (SOFC) produces electricity efficiently through the conversion of chemical energy which uses hydrogen and oxygen without compromising the environment. Development of SOFCs has recorded a technical peak and it is evident that hydrogen driven systems could replace fossil fuel-based combustion systems in transportation, stationary and distributed power systems in the near future [2]. Problems that include a lack of sustainable hydrogen resources, efficiency, affordability and reliable fuel processing systems as well as issues pertaining to hydrogen storage have continued to hinder its full commercialization [3, 4].

Therefore, there is a need to explore more reliable and sustainable energy sources for energy diversification. Indicators revealed that biomass, if properly utilized, could maintain a high level of energy production for future needs. This is not only due to its inherent potential as an energy reserve, but also due to its renewability, sustainability, biodegradable nature, even distribution and other environmental benefits [5]. The success recorded in the transesterification of vegetable oil to biodiesel has led to growth in the biodiesel industry which has left an excess of the by-product glycerol; this in turn exceeds its demand and is being considered a waste product [6]. By-product glycerol lacks good fuel properties to burn in petrol or diesel engines and it does not have the required purity to be useful for conventional uses of glycerol in cosmetics, pharmaceutical, food industries or

synthesis of other chemicals. More so, its disposal renege the environment. Interestingly, glycerol is biodegradable and an intense energy resource [7]. Because SOFCs operate at high temperatures and have flexibility regarding fuel choice, extensive research is focusing on using different processes for hydrogen production from biomass materials. These include liquid glycerol for the direct utilization of SOFCs or with little processing by way of reforming. Such reforming processes include steam reforming, partial oxidation and auto thermal reforming [8, 9].

Glycerol has demonstrated great potential for hydrogen production using steam reforming as seen in several theoretical equations as follows:

$$C_3H_8O_3 + 3H_2O \leftrightarrow 3CO_2 + 7H_2 + 128KJ/mol \quad \text{Eqn1}$$

$$C_3H_8O_3 \rightarrow 3CO + 4H_2 + 251\ KJ/mol \quad \text{Eqn2}$$

$$CO + H_2O \leftrightarrow CO_2 + H_2 - 41KJ/mol \quad \text{Eqn3}$$

$$CO_2 + H_2 \leftrightarrow CO + H_2O + 38kJ/mol \quad \text{Eqn4}$$

$$CH_4 + H_2O \leftrightarrow CO + 3H_2 + 206kJ/mol \quad \text{Eqn5}$$

$$CO_2 + 4H_2 \leftrightarrow CH_4 + 2H_2O - 165\ kJ/mol \quad \text{Eqn6}$$

$Ni/\gamma\text{-}Al_2O_3$ is a popular and promising catalyst system for steam reforming essentially due to nickel's propensity for C-C, C-H and H-O bond cleavages, high selectivity for syngas, cheap and ready availability. Gamma alumina is a good material widely used as a catalyst support or adsorbent due to its mesoporosity, ordered sponge-like pore structure, thermal stability and large surface area that could reduce coke formation and enhance diffusivity of reacting species and resulting products [10, 11]. As such, a lot is reported on the use of Ni-based catalyst for steam reforming of biomass materials [12, 13]. The major setback in the use of Ni based catalyst is deactivation due to carbon deposition and sintering at high temperatures. Some side reaction that could lead to coking includes but not limited to:

$$2CO \leftrightarrow CO_2 + C - 171.5\ KJ/mol \quad \text{Eqn7}$$

$$CH_4 \leftrightarrow 2H_2 + C - 75\ KJ/mol \quad \text{Eqn8}$$

$$CO + H_2 \leftrightarrow H_2O + C - 131\ KJ/mol \quad \text{Eqn9}$$

In this study, we explored the catalytic behavior of $Ni/\gamma\text{-}Al_2O_3$ in steam reforming of glycerol through tailoring of parameters such as catalyst loading, reaction and calcination temperature to enhance catalytic activity and reduce fouling of catalysts surface and consequent deactivation as results of carbon deposition or agglomeration.

2 Materials and Methods

2.1 Synthesis of Ni/Al_2O_3 Catalyst System

The supported catalysts were prepared using the wet impregnation method. $\gamma\text{-}Al_2O_3$ powder was dehydrated at 700 °C at a rate of 5°C/min for 5 hours to remove adsorbed moisture and gases before suspension in aqueous solution containing $Ni(NO_3)_2.6H_2O$ at 60 °C under stirring for 5 hours. The colloid solution was dried on a hot plate at 80 °C and dried overnight in an oven at 80 °C. The samples were pulverized and then air calcined at different temperatures ranging from 300-1000 °C at a heating rate of 5°C/min for 5 hours. After cooling, the powder was pulverized further and kept for additional analysis.

2.2 Catalyst Characterisations

Micrometrics TriStar II model was used to determine the Brunauer-Emmett-Teller (BET) surface area, Barret-Joyner-Halenda (BJH) pore volume and size using nitrogen adsorption/desorption at 77.35K. Each sample was degassed at 120°C for 3hrs before the analysis.

Crystallographic studies were carried out using Pan-Analytical Empyrean X-Ray Diffractometer operating on reflection mode using Cu-$K\alpha_1$ radiation at $\lambda = 1.5406$ Å and 10-90 2θ angle range for 1 hour.

Dispersion and morphology of Ni particles on the surface of the alumina was investigated using Field Emission Scanning Electron Microscopy (FESEM) JEOL JSM6700F micrographs using the Backscatter Method. The surface of each sample was coated with gold using Quorum Technologies Q150R instrument to enhance conductivity prior to the introduction into the SEM .

Used catalysts were analyzed for carbon deposition by temperature programmed oxidation (TPO) using NETZSCH STA 449C trigravimetric analyzer equipped with Thermostar mass spectrometer. After putting a known weight of the used catalyst into the TGA instrument, the system was flushed with argon to dispose of any other gas in the system. Oxidation of the surface carbon was done using O_2 gas and increased gradually 900 °C. Gases

Table 1: BET analysis showing how physicochemical properties changes with (a) catalyst loading, (b) calcination temperature.

Catalyst	Calcination Temperature °C	BET (m^2g^{-1})	Pore volume (cm^3g^{-1})	Pore diameter (nm)
Fresh Al_2O_3	-	76.64	0.31	20.33
Dehydrated Al_2O_3	700	74.46	0.37	25,50
5wt%Ni/Al_2O3	500	49.76	0.38	34.60
10wt%Ni/Al_2O_3	500	48.74	0.39	37.12
30wt%Ni/Al_2O_3	500	42.86	0.45	40.41
Catalyst	**Calcination Temperature °C**	**BET (m^2g^{-1})**	**Pore volume (cm^3g^{-1})**	**Pore diameter (nm)**
10wt%Ni/Al_2O_3	300	54.23	0.42	33.22
10wt%Ni/Al_2O_3	500	48.78	0.39	37.12
10wt%Ni/Al_2O_3	900	41.62	0.35	39.25
10wt%Ni/Al_2O_3	1000	36.10	0.32	44.67

generated were directed to the mass spectrometer for detection.

2.3 Catalyst Testing

Steam reforming of pure glycerol was carried out in a fixed quartz tube (10mm outer diameter (OD), 8mm inner diameter (ID) and 25cm long) at 300, 500, 600, 700 and 800 °C at atmospheric pressure (standard pressure). The glycerol/water mixture was supplied using a syringe Harvard apparatus 22 infusion pump at the flow rate of 0.019ml/min to a stainless steel pipe wrapped with a heating tape at 250 °C for vaporization and gas mixing. The vaporized reactant mixture was conveyed into the reactor by a carrier gas (Helium) at a flow rate of 40 ml/min and using H_2O/C =3. Gaseous products were analyzed using GC equipped with TCD (HP 6890 series) and a mass spectrometer residual gas analyzer.

3 Results and Discussion

3.1 Catalyst Characterization

Results of surface area analysis in Table-1a show that dehydration due to calcination at 700 °C reduced the surface area of the fresh γ-Al_2O_3 from 76.64 m^2g^{-1} to 74.46 m^2g^{-1} and resultant phase transformation from hydroxide to an active form of γ-Al_2O_3 as corroborated by the XRD pattern in Figure 2b. In Table 1a, the addition of active component NiO particles on the surface of the dehydrated alumina by wet impregnation progressively reduced the surface area of the γ-Al_2O_3 support as the loading increased. This indicates that active components have covered specific proportions of the surface of γ-Al_2O_3 support resulting in the dispersion of the active phase on the γ-Al_2O_3 support as evident in the SEM micrograph in Figure 1 below. Table 1b revealed that the surface area also progressively reduced as the calcination temperature increased from 300-1000 °C due to particle size growth and agglomeration at high temperatures. There is a progressive increase in pore volume with an increase in the catalyst loading in Table 1 attributable to the piling up or lumping of the catalyst , thereby making the pore volume larger. The pore volume is reduced in Table 2 and is constricted due to the influence of temperature.

The diffraction peaks for both NiO and active γ-Al_2O_3 were observed in the samples XRD pattern as indicated below in Figure 2a. The two most noticeable peaks at 46°, 68° and a wider one at 37° confirms γ-Al_2O_3 and their presence at all calcination temperatures as seen in Figure 3 signifying stability of γ-Al_2O_3.

The increase in the intensity of the alumina peak at 37° with an increase in nickel loading (from 5-30%) shows an overlap of the nickel peak with the alumina peak which depicts a possible formation of the spinel $NiAl_2O_4$ structure. The peak due to the spinel $NiAl_2O_4$ becomes more evident at 1000 °C in Figure 3 due to its temperature dependency. More so, in the same figure, the loss of NiO at 45°, 78° and 80° at high temperatures of 900-1000 °C leaves only peaks corresponding to $NiAl_2O_4$ has further support phase transformed to $NiAl_2O_4$ at high temperature.

In Figure 3, the XRD of Ni/Al_2O_3 catalyst shows the effect of calcination temperatures intensity of the Al_2O_3 peaks as they become sharper at high temperature of 900 °C and increase in intensity at 1000 °C indicating crystallinity

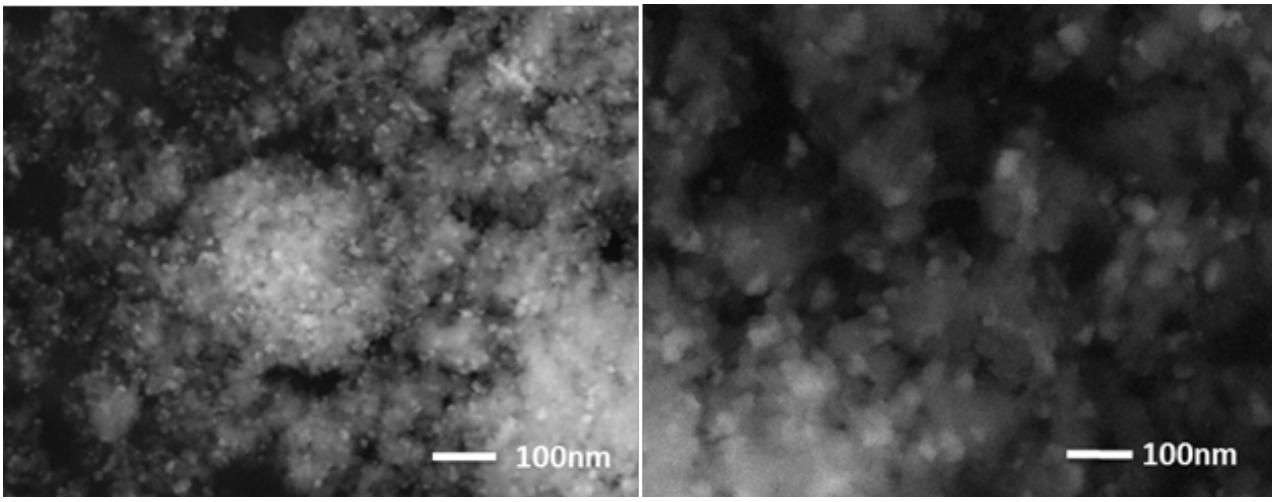

Figure 1: FESEM micrograph showing nickel particle dispersion on the γ-Al_2O_3 support

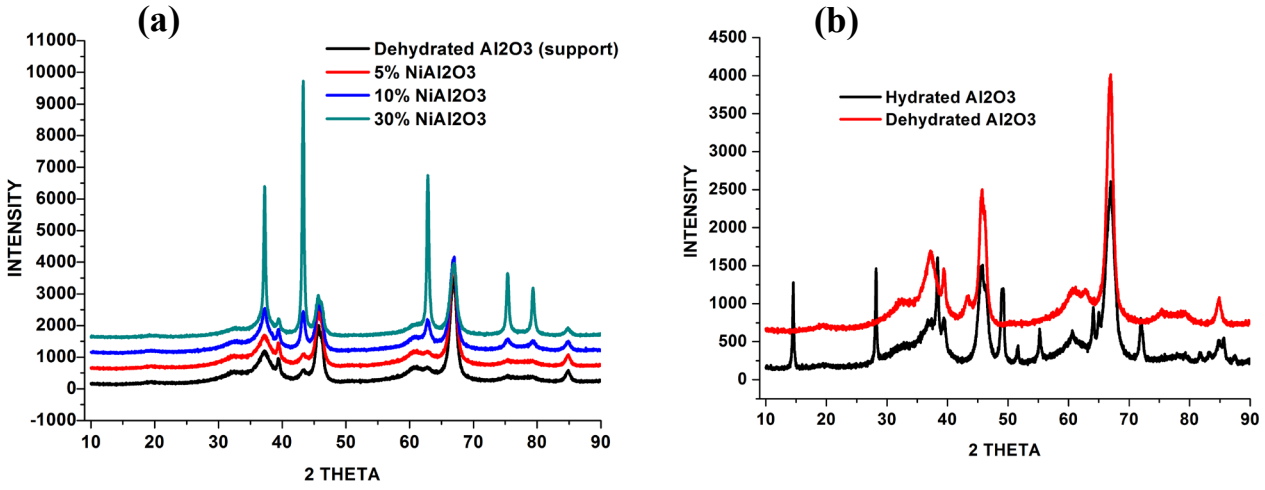

Figure 2: The XRD patterns of Ni/γ-Al_2O_3 catalyst systems showing **(a)** Effect of catalyst loading **(b)** transformation of the fresh hydroxide form of Al_2O_3 support to active form after dehydration at 700 °C.

Table 2: Influence of catalyst loading on crystallite size based on the longest NiO peak.

Sample	Calcination Temperature (°C)	Crystallite Size (nm)
5wt%Ni/Al_2O_3	500	14.5
10wt%Ni/Al_2O_3	500	20.2
30wt%Ni/Al_2O_3	500	45.0

of Al_2O_3 and a change of phase from amorphous γ-Al_2O_3 to a more crystalline α-Al_2O_3-like material such as θ-Al_2O_3 [14]. Different calcination temperatures exhibit different colors of the Ni/Al_2O_3 catalyst systems. 300 °C show a dark grey color, at 500 °C the color is light grey, at 900 °C the color is light blue and at 1000 °C the color is a deep blue. Color changes may be attributed to different states of nickel oxidation in the different nickel compounds formed in samples aside $NiAl_2O_4$ due to temperature changes (though not fully investigated in this work) which could also be used as an index for the extent or strength of metal-support interaction. Such color exhibition was reported by Kim et al [11]. Observed increases in peak intensity with an increase in nickel loading could be caused by the lumping or piling up of nickel particles as confirmed in the result of crystallite size calculation using Debye-Scherrer's equation below in Table 2.

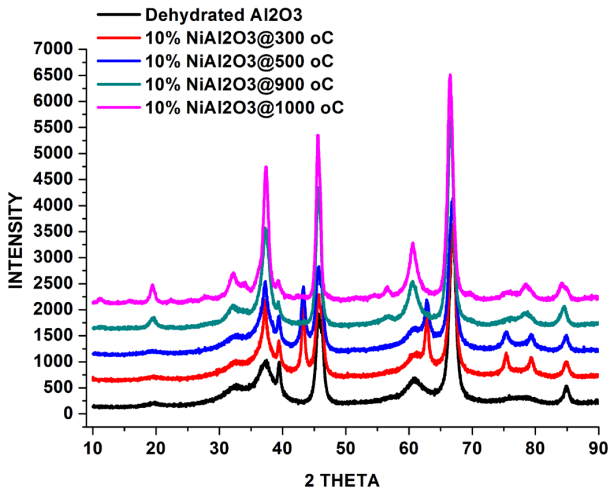

Figure 3: The XRD of Ni/Al_2O_3 catalyst showing effect of calcination temperatures.

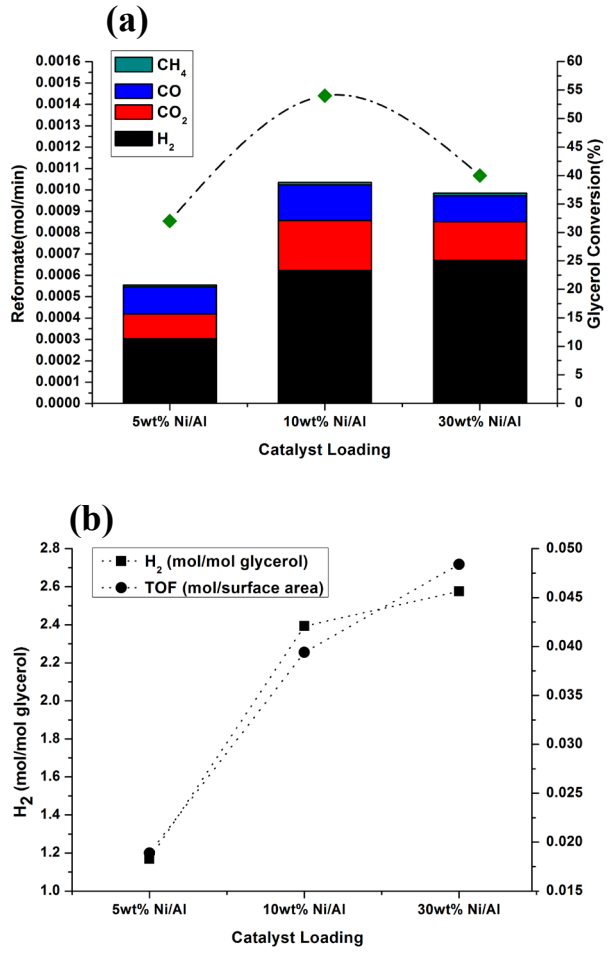

Figure 4: Show catalytic activity comparing **(a)** glycerol conversion to reformate (mol/min) in parallel with glycerol conversion (%) produced and **(b)** Hydrogen selectivity (mol/mol glycerol) to turn over frequency (mol/surface area).

3.2 Catalyst Test

3.2.1 Catalyst Activity in relation to Catalyst Loading

To evaluate performance of the catalysts containing different Ni loading, a reforming test was carried out at 500 °C using catalysts prepared at 500 °C calcination temperature, but containing different catalyst loading at the weight hourly space velocity (WHSV) of 28 h^{-1}. The results of the catalyst test based on 100mg of the catalyst amount in the reactor revealed that catalyst activity taken as glycerol conversion to gaseous products and product distribution increased with catalyst loading from 5wt% to 10wt% and decreased at 30wt% as shown in Figure 4a. As the loading increased to 30wt%, the drop in conversions could be attributed to the reduced surface area and particle size growth due to nickel particles piling up as exhibited in Table 1a and Table 2. This may have reduced the surface active site accessibility leading to a decrease in surface reaction. Therefore, 10wt% catalyst loading represents the optimum catalyst (NiO) loading for a maximum catalyst conversion in this work. The product distribution shows H_2, CO_2, CO, and CH_4 as the only gaseous products detected during the steam reforming of glycerol at such temperatures. H_2 and CO_2 were the predominant products with high readings of CO.

The product distribution suggests catalytic decomposition due to nickel's propensity for glycerol C-C cleavages which could be responsible for the high CO content. Other reactions that contribute to the observed performance include a water gas shift reaction (WGSR) as shown in the equations above. Furthermore, hydrogen production per mole glycerol increased with catalyst loading. The hydrogen was about 60% of the equilibrium composition with 10wt% catalyst which increased to 66% with 30wt% catalyst loading. The turnover frequency which expresses the number of molecules that react per surface area of the catalyst shows reasonable value corroborating the usefulness of the catalyst system under these conditions for hydrogen and syngas production.

3.2.2 Correlation between Reaction Temperature and the Catalytic Behaviour.

The influence of the reaction temperature was investigated using 10wt% Ni/Al_2O_3 calcined at 500 °C which gave the highest conversion of glycerol in the screening test seen in Figure 4. The test was carried out at different reaction temperatures between 500-800 °C using the S/C ratio of 3 and WHSV of 28 h^{-1}. The graph below in Figure 5a

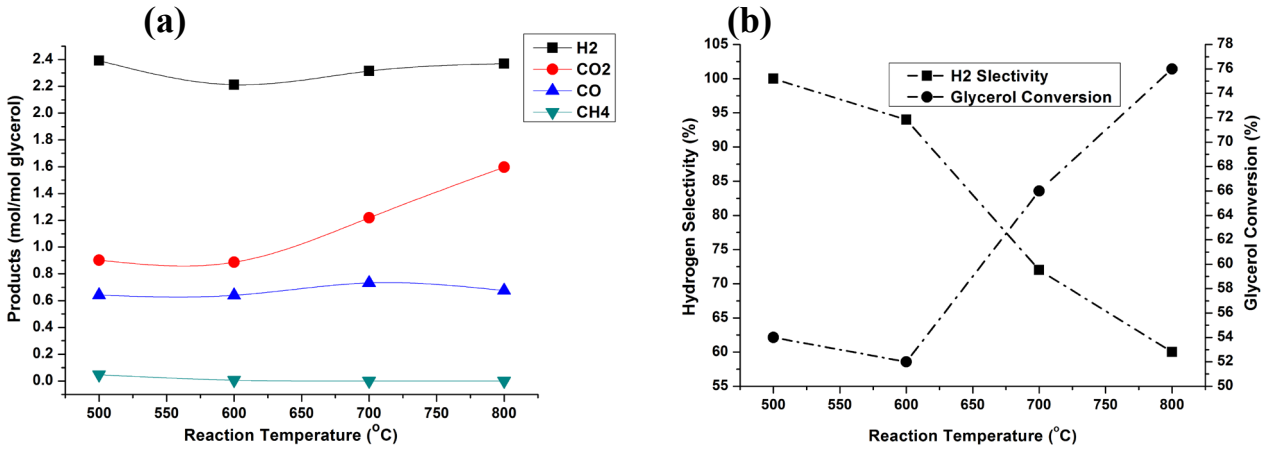

Figure 5: **(a),** Change in reformate composition with temperature **(b),** Comparison between hydrogen selectivity and glycerol conversion and influence of reaction temperature.

illustrates product distribution changes with temperature. The results based on 100mg catalyst amount in the reactor show that reaction kinetics influenced by temperature play an important role in the product distribution. This is attributable to enhanced rapid glycerol decomposition due to kinetics. H_2 and CO_2 yield was high at 500 °C which may be due to a water gas shift reaction (WGSR) since is slightly exothermic (Eqn3). There was a simultaneous decrease in CO and CH_4 at the same temperature (500 °C) because CO was used in the WGSR and CH_4 decomposition to yield more H_2 in a slightly exothermic reaction (Eqn8). H_2 and CO_2 yield dropped at 600 °C with a corresponding stabilization of CO and CH_4 formation or yield. This suggests, as the temperature increased, a reverse water gas shift reaction which is slightly endothermic and which favors a CO formation by consuming CO_2 and H_2.

The drop in H_2 and CO_2 at 600 °C is attributable to a reversible self-poisoning deactivation effect which occurs most frequently at 550-600 °C [15]. The observed increase in CO with temperature is also an indicator of catalyst deactivation. At high temperatures, highly endothermic steam reforming and glycerol decomposition favored a rise in H_2 and CO_2 selectivity, while CO and CH_4 decreased. The CO rise from 600 °C-700 °C could be attributed to methane reforming which is a highly endothermic reaction. These findings relate to the thermodynamic observations [16, 17]. Figure 5b shows how a change in reaction temperature influences H_2 selectivity and how that compares with glycerol conversion at different temperature in reverse trend. Glycerol conversion decreased at 600 °C from 500 °C but increased steadily to 800 °C. Conversely, hydrogen selectivity decreased progressively as temperatures rose to 800 °C as evident in Figure 5b. This could be due to the increased glycerol decomposition and the reforming process as both are highly endothermic processes (Eqn1&2). Carbon deposition also decreased with temperature as seen in section 3.3.1 which might have favored a glycerol conversion. It is evident that temperature enhances rapid glycerol decomposition and glycerol conversion; however, hydrogen production and selectivity did not show a noticeable increase at high temperatures. 500 °C represents the optimum reforming temperature with the 10wt% Ni/Al_2O_3 catalyst system in this work.

3.2.3 Influence of calcination temperature on the steam reforming

Both reaction temperatures and calcination temperatures of the catalyst has profound influence on the selectivity of the desired products. The test was carried out under the same reaction conditions as stated in section 3.2.2. Figure 6 shows that the catalyst prepared at a low temperature had a better selectivity for hydrogen than the one prepared at high calcination temperatures. The catalyst prepared at 300 °C showed a steady increase in hydrogen selectivity with an increase in reforming temperatures. In contrast, the catalyst prepared at 500 °C showed a steady decrease in hydrogen selectivity as the reaction temperature increased. This is attributable to the change in surface morphology and chemistry with increase in reaction temperature. It is apparent that H_2 and CO_2 yield is better among catalysts calcined at low temperatures, which suggests they are good for WGSR. This may be due to their better surface area, smaller particle size and good catalyst-support interaction. Relatively, due to sintering and agglomeration, those catalysts prepared at high temperatures-900-100 °C favor reverse water

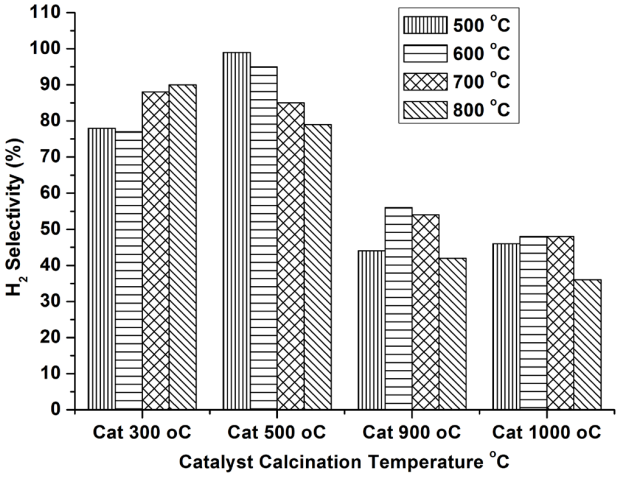

Figure 6: Influence of calcination and reaction temperature on hydrogen selectivity.

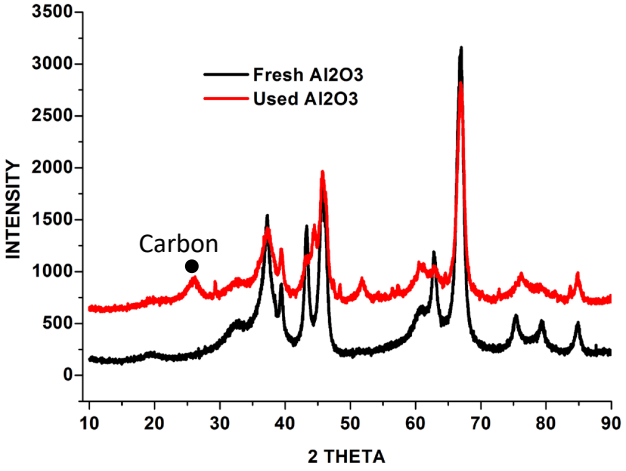

Figure 7: Comparison of the XRD pattern of fresh catalyst containing 10% $NiAl_2O_3$ calcined at 500 °C and used catalyst systems after the catalysis at 500 oC using the same catalyst showing peak due to carbon on the used catalyst.

gas reaction, hence reduced H_2 and CO_2 and increased CO and CH_4 formation. Consequently, low calcination temperatures (300-500 °C) favor maximum hydrogen yield and selectivity.

3.3 Carbon deposition

Post catalysts test investigation on the XRD pattern of the used catalyst samples (Ni/γ-Al_2O_3) in Figure 7 shows a peak at 26.2 2θ which remains absent in the fresh Ni/γ-Al_2O_3. The peak corresponds to carbon which suggests carbon deposition. A similar observation was made by Newnham et al [18].

More so, peaks due to Ni metal are prominent at 52.1 2θ and 76.6 2θ in the XRD pattern of the used catalyst as a result of reduction of the catalyst before use compared to the fresh sample pattern with peaks due to NiO only. Temperature programmed oxidation (TPO) analysis on the used samples showed one or more CO_2 peaks that corresponded to the temperature at which coke oxidation occurred. Different types of coke such as graphitic, polymeric or amorphous carbon are oxidized at different temperatures. The TPO profile could be used to characterize the coke deposited. Moreover, depending upon the position of the major CO_2 peak, the point or particular place on the catalyst surface where the bulk of the carbon is deposited, could be determined. Low temperature peaks correspond to amorphous coke deposited on the Ni active phase or metal centres; medium temperature peaks correspond to polymeric or graphitic coke deposited at metal-support interface while high temperature CO_2 peaks signify carbon or coke deposited on the support [19].

3.3.1 Influence of reaction temperature on coke deposited

Figure 8 shows the TPO profiles obtained from oxidation of used catalyst calcined at 500 °C; but they ran at different temperatures between 500-800 °C for the steam reforming. It is evident that the extent or amount and type of coke deposited was affected by changing the reaction temperature. At intermediate reaction temperatures between 500 and 600 °C,a major CO_2 peak was detected at 500-520 °C. This indicated that the bulk of the coke was polymeric or graphitic and deposited at the metal-support interface. The small CO_2 peak detected at low temperature shows that oxidation starts at a low temperature. Table 3 summarizes the peak positions as seen in Figure 8. Conversely, high temperature reforming between700-800 °C is characterized by low, intermediate and high temperature peaks with the dominant peaks at low temperatures indicating that most of the carbon was deposited on the active phase (Ni) and is an amorphous type usually easy to remove and could be regenerated by oxidation. The extra peaks at intermediate and high temperatures suggest a presence of polymeric or graphitic carbon as well as bulk carbon which are difficult to remove and therefore, oxidize at higher temperatures.

The TGA profile showed a decrease in carbon deposition with an increase in reforming temperatures

Table 3: CO_2 peak positions showing temperatures at which different types carbon were oxidized.

Catalyst	Reaction Temp. °C	Low Temp Peak	Medium Temp Peak	High Temp Peak
10wt%Ni/Al_2O_3	500	290	540	-
10wt%Ni/Al_2O_3	600	290	540	-
10wt%Ni/Al_2O_3	700	320	550	660
10wt%Ni/Al_2O_3	800	260	580	640

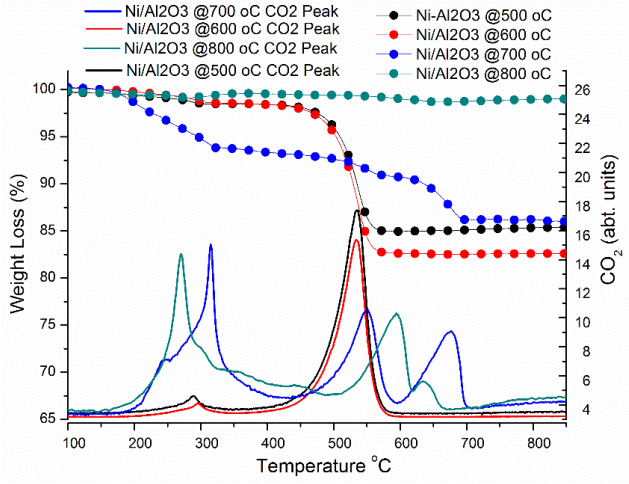

Figure 8: Change in weight of the selected used catalyst samples in oxidising atmosphere monitored in parallel with CO_2 as a function of temperature.

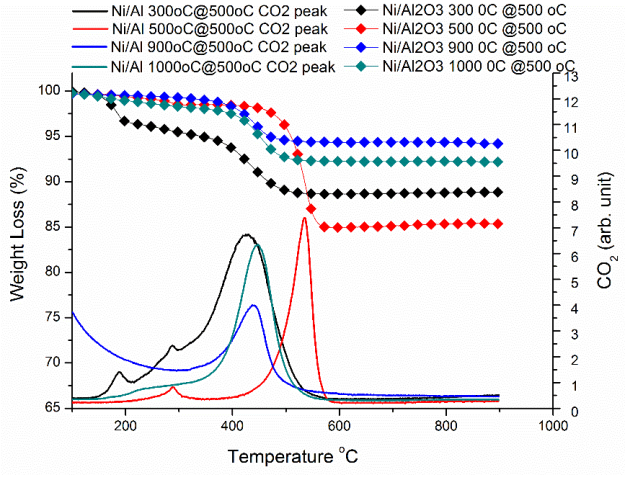

Figure 9: Change in weight of the selected used catalyst samples in oxidising atmosphere monitored in parallel with CO_2 as a function of temperature.

which proved that carbon deposition was indeed limited by temperature as suggested in Eqn7-9 above. The equations show that the reactions leading to carbon deposition are exothermic and therefore favored at low temperatures and hindered at high temperatures. At a reaction temperature of 800 °C, carbon deposition was almost completely hindered which aligns with thermodynamic observations [16, 17]. The catalyst used at a reaction temperature of 600 °C gave the highest carbon deposition which is attributable to the occurrence of side reactions due to the self-poisoning effect highlighted above which led to catalyst deactivation. Generally, the carbon deposition was about 16% and the highest at 600 °C. The acidic Al_2O_3 support surface attracted a large amount of glycerol to its surface leading to the formation of carbonaceous products that could lead to deactivation.

3.3.2 Influence of calcination temperature on carbon deposition

Figure 8 shows how calcination temperature influences the quantity and type of coke deposited. The catalysts were prepared at different temperatures of 300 °C, 500 °C, 900 °C and 1000 °C respectively and tested for steam reforming at a constant temperature of 500 °C. TPO on the used catalyst was analyzed, and the results are shown in Figure 8. The major CO_2 peak is a medium temperature type, although the catalyst calcined at lower temperatures show some lower temperature peaks. The carbon is more graphitic with the catalyst calcined at 500 °C due to the intense surface reaction it attracted. Others gave polymeric carbon, hence the CO_2 peak occurred at a slightly lower temperature. The lower temperature catalysts had more carbon deposition compared to the high temperature catalysts in reference tothe TGA profile. This might be due to their large surface area and higher glycerol adsorption; therefore intense surface reactions could leave behind more carbon deposition. Table 4 summarises the peak positions as per Figure 9.

4 Conclusion

Ni/γ-Al_2O_3 catalyst was successfully synthesized containing different Ni loading by wet impregnation and the catalytic performance in steam reforming of glycerol was evaluated. H_2 yield and selectivity increased with an increase in the catalyst loading up to 30wt%, while the glycerol conversion increased to 10wt% and

Table 4: CO_2 peak positions showing temperature at which carbons were oxidized.

Catalyst	Calcination Temp. °C	Low Temp Peak (°C)	Medium Temp Peak (°C)	High Temp Peak (°C)
10wt%Ni/Al_2O_3	300	280,180	420	-
10wt%Ni/Al_2O_3	500	280	540	-
10wt%Ni/Al_2O_3	900	-	450	-
10wt%Ni/Al_2O_3	1000	-	450	-

dropped at 30%. Hence, 10wt% nickel catalyst loading is the optimum catalyst loading for maximum glycerol conversion. Both reaction and calcination temperature have profound influence on steam reforming of glycerol. Lower reforming temperature-500 °C favor water gas shift reaction to yield more H_2 and CO_2, while high reforming temperatures between 700-800 °C favour reverse water gas shift reaction, hence the domination of CO and CH_4. Phase transformation of the catalyst to spinel specie $NiAl_2O_4$ occurred at higher temperatures between 900-1000 °C. The $NiAl_2O_4$ formation, agglomeration and carbon deposition were identified as the main agents of deactivation. Reforming and calcination temperatures affect both extent and the type of carbon that was deposited. At low reforming temperatures of 500-600 °C, most of the carbon was polymeric carbon and deposited at metal-support interface. High reaction temperatures were predominantly characterized by amorphous carbon depicted by the low temperature CO_2 peak deposited on the active phase (Ni). There is also little polymeric or graphitic carbon at the metal-support interface shown by the medium temperature CO_2 peak as well as bulk carbon represented by the higher temperature CO_2 peak deposited on the support at higher temperature. The amount of carbon deposited decreased with an increase in reaction temperature as well as calcination temperature. Calcination temperature did not have an influence on the type of carbon except for the carbon being more graphitic as the active catalyst calcined at 500 °C. Hence, catalyst loading, calcination and reaction temperatures could be tailored to enhance structural and catalytic properties as well as suppress the carbon deposition to mitigate catalyst deactivation.

Acknowledgements: I thank the Petroleum Technology Development Fund (PTDF), Nigeria for funding this research and the University of St Andrews, Scotland UK for the consideration to work with them and to use their facilities.

References

[1] Dorian, J. P., Franssen, H. T., Simbeck, D. R., (2006). Global challenges in energy. *Energy Policy* **34**, 1984–1991.

[2] Cimenti, M., Hill, J. M., (2009). Direct utilization of liquid fuels in SOFC for portable applications: Challenges for the selection of alternative anodes. *Energies* **2**, 377–410

[3] Shekhawat, D., Spivey, J. J., Berry, D. A., (2011). Fuel Cells: *Technologies for fuel processing*. Elsevier, 1-43.

[4] Edwards, P. P., Kuznetsov, V. L., David, W. I. F., Brandon, N. P., (2008). Hydrogen and fuel cell: Towards sustainable energy future. *Energy Policy*, **38**, 4356-4362.

[5] Saxena, R. C., Adhikari, D. K., Goyal, H. B., (2009). Biomass-based energy fuel through biochemical routes: A review. *Renewable and Sustainable Energy Reviews,* **13**, 167–178.

[6] Demirbaş, A., (2003). Biodiesel fuels from vegetable oils via catalytic and non-catalytic supercritical alcohol transesterification and other methods: a survey. *Energy Conversion and Management*, **44**, 2093–2109.

[7] Lo Faro, M., Minutoli, M., Monforte, G., Antonucci, V., Aricò, A. S., (2011). Glycerol oxidation in solid oxide fuel cells based on a Ni-perovskite electrocatalyst. *Biomass and Bioenergy* **35**, 1075–1084.

[8] Balat, H., Kırtay, E., (2010). Hydrogen from biomass – Present scenario and future prospects. *International Journal of Hydrogen Energy,* **35**, 7416–7426.

[9] Kırtay, E., (2011). Recent advances in production of hydrogen from biomass. *Energy Conversion and Management,* **52**, 1778–1789.

[10] Sanchez, E. A., Comelli, R. A., (2012). Hydrogen by glycerol steam reforming on a nickel–alumina catalyst: Deactivation processes and regeneration. *International Journal of Hydrogen Energy*, **37**(19) doi:10.1016/j.ijhydene.2011.12.088.

[11] Kim, Y., Kim, P., Kim, C., Yi, J., (2003). A novel method for synthesis of a Ni/Al_2O_3 catalyst with a mesoporous structure using stearic acid salts. *J. Mater. Chem.* **13**, 2353–2358.

[12] Seo, Y., Jung, Y., Yoon, W., Jang, I., Lee, T., (2011). The effect of Ni content on a highly active Ni-Al_2O_3 catalyst prepared by the homogeneous precipitation method. *Int. j. of hydrogen energy,* **36** 94-102.

[13] Fiuza, R. D., Da Silva, M. A., Boaventura, J. S., (2010). Development of Fe-Ni/YSZ-GDC electrocatalyst for application of SOFC anodes: XRD and TPR Characterization and evaluation in the ethanol steam reforming reaction. *Int. j. of hydrogen energy* **35** 11216-11228.

[14] Perego, C., Villa, P., (1997). Chapter 3 Catalyst preparation methods. *Catalysis Today,* **34**, 281–305.
[15] Breen, J. P., Burch, R., Coleman, H. M., (2002). Metal-catalysed steam reforming of ethanol in the production of hydrogen for fuel cell applications. *Applied Catalysis B: Environmental*, **39** 65–74.
[16] Da Silva, A., Muller, I. L., (2010). Operation of solid oxide fuel cells on glycerol fuel: A thermodynamic approach using Gibbs free energy minimization approach. *J. of power energy,* **195**, 5637-5644.
[17] Adhikari, S., Fernando, S., Gwaltney, R. S., To, S. D. F., Bricka, R. M., Steele, P. H., Haryanto, A., (2007). A Thermodynamic analysis of hydrogen production by steam reforming of glycerol. *Int. j. Hydrorgen Energy,* **32**(14), 2875-80.
[18] Newnham, J., Mantri, K., Amin, M. H., Tardio, J., Bhargava, S. K., (2012). Highly stable active Ni-mesoporous alumina catalysts for dry reforming of methane. *Int. j. of hydrogen energy,* **37**, 1454-1464.
[19] Mawdsley, J. R., Krause, T. R., (2008). Rare earth-first-row transition metal perovskites as catalyst for the auto thermal reforming of hydrocarbon fuels to generate hydrogen. *Applied catalysis A. General* **334** 311-320.